



# Impact of Energy Storage Devices on the Distribution System Stability with Distributed Generation

## تأثير أجهزة تخزين الطاقة على إستقرار منظومة توزيع القوى الكهربائية في وجود مصادر توليد موزعة

Mohamed Talal, Sahar Kaddah and Abdelfattah Eladl

### KEYWORDS:

photovoltaic systems, energy storage, batteries, SMES, power system stability

*الملخص العربي:* تتمتع مصادر الطاقة المتجددة بمزايا بيئية واقتصادية، ولكنها تتسبب في العديد من التغيرات والمشاكل الحادة في منظومة القوى. ومن بين الحلول التي قد تساعد في الحد من هذه المشاكل تصميم المصادر المتجددة كمولدات موزعة في منظومة توزيع الطاقة. من الضروري إضافة أنظمة تخزين الطاقة إلى منظومة القوى لتحسين تأثير المولدات الموزعة على استقرار نظام الطاقة. في هذا البحث، تم إضافة خلايا شمسية مزودة بأجهزة لتخزين الطاقة مثل البطاريات ونظام تخزين الطاقة المغناطيسي فائق التوصيل إلى منظومة التوزيع وتحليل استقرار المنظومة باستخدام برنامج محاكاة (MATLAB/Simulink®). تتم دراسة الاستقرار العابر لمنظومة القوى بناءً على العديد من العوامل مثل الحد الأقصى لانحراف سرعة الدوران، والانخفاض في جهد الشبكة والانخفاض في جهد المستمر للنظام الكهروضوئي. يتم محاكاة حالات غير طبيعية مختلفة لإظهار تأثير تكوين النظام على استقراره. وتم عمل دراسة مقارنة للتحقق من صحة النتائج. تبين أنه يتم تحسين استقرار نظام الطاقة من خلال إضافة الخلايا الكهروضوئية ويزداد عن طريق إضافة أنظمة تخزين الطاقة.

**Abstract**—Renewable energy sources have environmental and economic advantages, but it causes many fluctuations and severe problems on the power system. One solution to decrease these problems are designing renewable sources as distributed generations (DGs) on the power distribution system. But it is necessary to add energy storage systems (ESS) to the power system to improve the impact of DGs on the power system stability. In this paper, the photovoltaic system (PV) with energy storage devices such as battery or superconducting magnetic energy storage systems (SMES) is added to the power system and analyzed the stability of the system by using the software program, “MATLAB/Simulink®”. The transient stability of the power system is studied based on many factors as maximum rotor speed deviation, the drop-in grid voltage, and the drop in DC voltage of the PV. A different abnormal system states are simulated to show the effect of system configuration on its stability. For validation, a

comparative study is implemented. From the results, it is found that the stability of the power system is improved through the adding of the PV system and increased by adding energy storage systems.

### I. INTRODUCTION

CONVENTIONAL Power sources that used fossil fuels have a destructive environmental impact; because there are CO<sub>2</sub> emissions from these power plants. So it is very important to search for clean energy. CO<sub>2</sub> emissions are decreased with the addition of more renewable energy sources to the power grid. Nowadays, many types of renewable sources which are added to the power system like a wind turbine, solar cells, and geothermal energy, etc... Also, adding renewable energy sources to the electricity sector reduce

Received: (27 April, 2020) - Revised: (16 July, 2020) - Accepted: (17 July, 2020)

Mohamed Talal, a researcher at Mansoura university, faculty of Engineering, Electrical Engineering Department, Egypt, +201018521842, (e-mail: mohamed.eng73@yahoo.com).

Prof. Sahar S. Kaddah, Electrical Engineering Department, Faculty of Engineering Mansoura University, Egypt, she is the head of Electrical Engineering Department, +201221113475, (e-mail: skaddah@mans.edu.eg).

Dr. Abdelfattah A. Eladl, Electrical Engineering Department, Faculty of Engineering, Mansoura University, Egypt, +201227074312, (e-mail: eladle7@mans.edu.eg)

the use of fossil fuel which has a high cost. So, renewable energy sources have environmental and economic benefits. Although renewable energy sources have many benefits, they also have many drawbacks. Where its operation and efficiency depend on the state of the weather and it causes many fluctuations and reduces the stability of the power system. One solution to reduce the problems caused by renewable sources is to add them as a distributed generation (DG) to the power system [1]. Where DGs are small generators connected in the distribution system behind the load to supply the power system with a few MW. The power system becomes unstable with some of the abnormal conditions, but when DGs added to the network they can improve the stability of the system and also provide it with the necessary power [2]. The system which connected with DG requires an ideal operation and proper protection to make appropriate changes [3]. The DG can be a renewable source such as a photovoltaic cell or a nonrenewable source. The impact of solar cells on the power system stability depends on the continuity of providing the power system with the required power [4]. So, it is important to add the energy storage systems (ESS) to the solar system and using it with the increased loads. In addition to supply the solar system during peak loads, the ESS is used to smooth the output power of solar cells and improve the stability of the power system [5]. Nowadays, there are different technologies and applications of ESS such as a compressed air energy storage system, pumped hydro energy storage system, flywheels, ultra-capacitor energy storage device, battery energy storage system, and superconducting energy storage system (SMES). A detailed comparison of these different energy storage systems was presented in [4, 5]. The best type of batteries used with power systems is lead-acid batteries with efficiency 78% and is the best choice when compared between its performance and its cost, while on the other side, lithium-ion has better performance but more expensive [6]. Superconducting magnetic energy storage systems (SMES) which use a superconducting coil cryogenically cooled and DC passed through it to get stored energy in the form of a magnetic field [7]. SMES is made from superconductive wire so it has high efficiency and has a high cost [7]. The efficiency of SMES is very high about 90% because the energy doesn't convert from its formation to another form. Also, SMES can be used in increasing the stability of the power grid as well as controlling power flow [8]. The SMES increases the stability of the system quickly because it has a rapid response and with high energy density [9].

Power system stability (PSS) is a vital topic to investigate the performance of the power grid under disturbances. PSS is known as the ability of the power system to back to an acceptable equilibrium state after abnormal conditions. It can be measured by rotor angle stability which includes studying the oscillations of power systems, and voltage stability which indicates the condition of the electrical system to continue with acceptable limits of voltage at all buses after disturbances happen. The effect of the penetration level of PV on PSS and its location is given in [10], and the obtained results showed that the power system stability was improved when the generator near DG. Authors in [11] presented a comprehensive study of

the effect of increasing the penetration level of PV on transient stability and showed that it made a negative impact on PSS according to its results. In [12], the authors investigated the impact of PV with the normal operation of the power system but didn't discuss the effect of faults on the power system. In [13], the authors studied the effect of DG with ESS like battery and ultra-capacitor on the stability of the power grid with the technical and economic analysis. The technical analysis shows that, the energy storage devices made a great impact on the efficiency of the electrical system. And the economic study was done through the HOMER program tool and the obtained results showed that the energy storage systems reduced the use of fossil fuel which has a high cost. In [14] authors discussed the addition of solar cells to the electrical system and reviewed the technology of storing energy which can improve the performance of the grid, where the specifications of many energy storage devices not analyzed in detail in this research. The effect of ESS on the frequency stability of the grid was presented in [15] and showed that ESS could improve it. In [16] authors discussed the effect of the single-phase to neutral fault in the power system, where the system more stable during the single-phase to neutral fault than the three-phase fault. Also, the place of fault from the electricity source is one factor that has an impact on transient stability [16]. The effect of solar cells on the stability of the grid measured by the rotor angle was investigated in [17] and showed that the stability was improved by the addition of extensive PV generation to the grid, but this work did not analyze the great impact of storage systems with PV plants.

This paper focuses on the discussion of the impact of PV systems with ESS like conventional batteries/SMES on the stability of the distribution system at steady-state and at abnormal conditions. This research uses MATLAB/Simulink<sup>®</sup> to model a photovoltaic system connected with a modeled DC-DC boost converter which is used to obtain the maximum power by using the maximum power point tracking (MPPT) technique. Then, the boosted DC voltage is converted to AC voltage by using a three-phase inverter, where the solar system is connected with the radial distributed 8-bus system. The lead-acid battery and SMES are connected in a DC bus to study the stability of the power system. Different cases are presented to study the impact of the PV system with/without energy storage devices on the power system stability. Finally, the stability of the system is analyzed according to many indicators under different operation cases.

The main contribution of this paper can be briefly abbreviated as the following:

- Modeling the main components of the solar system with energy storage devices by using MATLAB/Simulink<sup>®</sup>.
- Analyzing the power system stability under abnormal conditions with the addition of PV and energy storage systems like batteries and SMES.

The paper is designed as the following: The Power system modeling and description is explained in part II. Part III discusses the problem-solving procedure. Section IV presents the case study and the results of power system stability. Finally, the conclusions are mentioned in part V.

**II. SYSTEM MODELING AND DESCRIPTION**

Abnormal conditions such as faults and load switching can cause undesirable states of the power grid and will decrease its stability. So, adding DGs with energy storage devices to the electric grid improves the performance of the network during faults and increases its reliability [13]. The power system under investigation contains a PV array which is modeled according to its equivalent circuit. These PV arrays attach with a boost converter which uses an MPPT technique. Then, the boosted DC voltage of the solar system is converted into a three-phase voltage by using a voltage source converter to obtain the reactive and active powers necessary for the network as shown in Fig.1. In this section, the detailed modeling of each system component is presented.

**A. PV array model**

PV array with nonlinear characteristics that proportional to

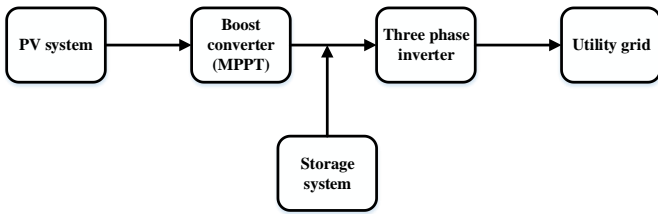


Fig. 1. schematic drawing of the simulated system.

solar irradiation and temperature is modeled by its I-V characteristics function [18-20]. PV arrays consist of solar cell modules linked in parallel and series to produce the suitable DC voltage. The photovoltaic cell is simulated as shown in Fig. 2 [23].

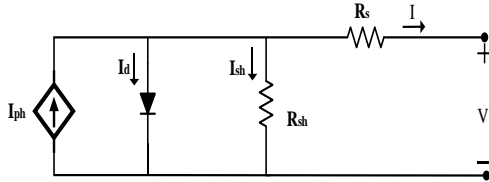


Fig. 2. The equivalent circuit of solar cell.

The mathematical model of the solar system is given depending on the following equations [24]:

$$I_{ph} = I_{rr} \left( \frac{K_i (T - 298) + I_{sc}}{1000} \right) \quad (1)$$

$$I_s = \exp \left[ \frac{Q E_{go}}{n k} \left( \frac{1}{T} - \frac{1}{T_r} \right) \right] \left( \frac{T}{T_r} \right)^3 I_{rs} \quad (2)$$

$$I_{rs} = I_{sc} / [\exp(Q V_{oc} / c k n T) - 1] \quad (3)$$

$$I = N_p \left( I_{ph} - I_{rs} \left[ \exp \left( \frac{V/N_s + I R_s / N_p}{n V_t} \right) - 1 \right] \right) - I_{sh} \quad (4)$$

$$I_{sh} = \left( I R_s + \frac{N_p}{N_s} V \right) \frac{1}{R_{sh}} \quad (5)$$

$$V_t = \frac{T K}{Q} \quad (6)$$

where,  $I_{ph}$  is the photo current of the cell (A),  $I_{rr}$  is the irradiation of the sun ( $W/m^2$ ),  $T_r$  is the rated temperature = 298.15 (K),  $I_{sc}$  is the short circuit current (A),  $k$  is the constant of Boltzmann =  $1.3805 \times 10^{-23}$  (J/K),  $I_{rs}$  is the saturated reverse current (A),  $I$  is the output current of the PV module (A),  $I_{sh}$  is the current which passed through shunt resistance,  $n$  is the ideality coefficient of the diode,  $R_s$  is the series resistance,  $I_s$  is the current of saturation (A),  $K_i$  is the factor of short-circuit current of the cell,  $T$  is the actual temperature (K),  $Q$  is the charge of the electron =  $1.6 \times 10^{-19}$  (C),  $V_{oc}$  is the open-circuit voltage (V),  $V$  is the output voltage (V),  $N_s$  is the number of series solar modules,  $V_t$  is the output terminal voltage (V),  $R_{sh}$  is the shunt resistance,  $E_{go}$  is the bandgap energy of the semiconductor = 1.1 (eV),  $C$  is the number of series cells,  $N_p$  is the number of solar modules connected in parallel.

As shown in Fig. 3 and Fig. 4 respectively, the I-V and P-V characteristics of the designed solar system in this paper are simulated at constant temperature and with variable irradiation. The parameters of the modeled solar cell, which present in this work are modified according to a real solar system (sun power SPR-305watts).

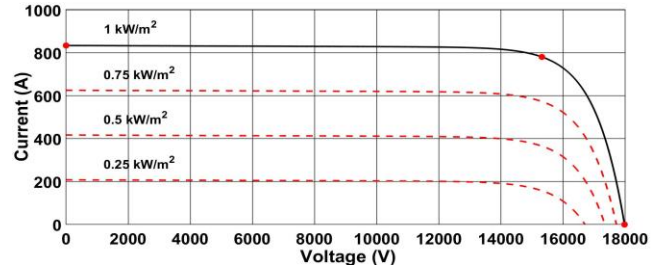


Fig. 3. I-V features of a photovoltaic system [25].

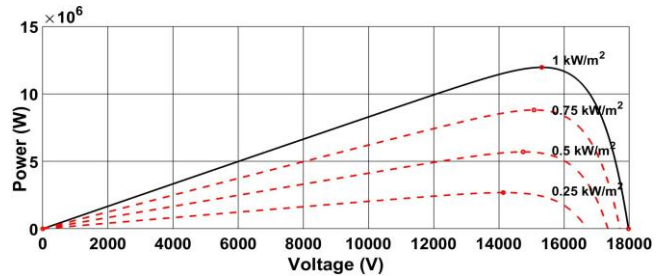


Fig. 4. (P-V) features of a photovoltaic system [25].

**B. Boost converter model**

The boost converter is added to the solar system for raising the output small voltage from the solar cell, so it called a step-up converter [21]. The converter uses an MPPT technique to track the maximum power by controlling the duty cycle, where the obtained voltage from the boost converter is expressed by the following equation [26]:

$$V_{out} = \frac{V_g}{1 - D} \quad , \quad D = \frac{T_{on}}{T} \quad , \quad \text{and} \quad T = \frac{1}{F} \quad (7)$$

where  $V_{out}$  is the output voltage from the boost converter,  $V_g$  is the DC voltage from the solar system,  $D$  is the duty cycle of the boost converter,  $T$  is the switching time, and  $T_{on}$  is on period.

Fig. 5 shows an equivalent circuit of a boost converter which consists of an inductor, filtering capacitor, diode, and the IGBT controlled switch [26].

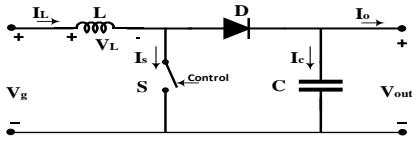


Fig. 5. Equivalent circuit of the boost converter.

### C. Maximum power point tracking (MPPT) model

The technique used with designing the MPPT system is called perturb and observe (P&O) method [21]. This algorithm observes the output voltage at the DC bus and the output power from the DC converter during varying the duty cycle of the boost converter [19]. This disturbance changes the output power of the solar system and continues in the direction of the increased power. When the power reached maximum value, perturbation is reversed and oscillate around the required point until it reaches to steady-state as shown in Fig. 6 [10, 21]. Fig. 7 indicates the flow chart of this technique [25].

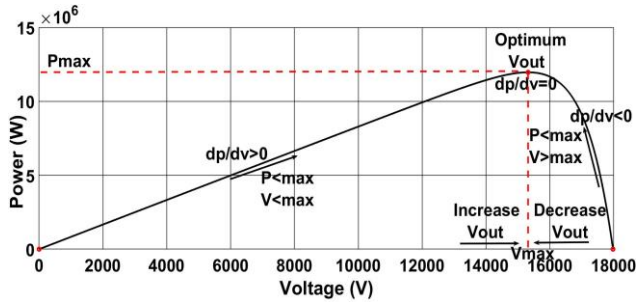


Fig. 6. MPPT operation technique.

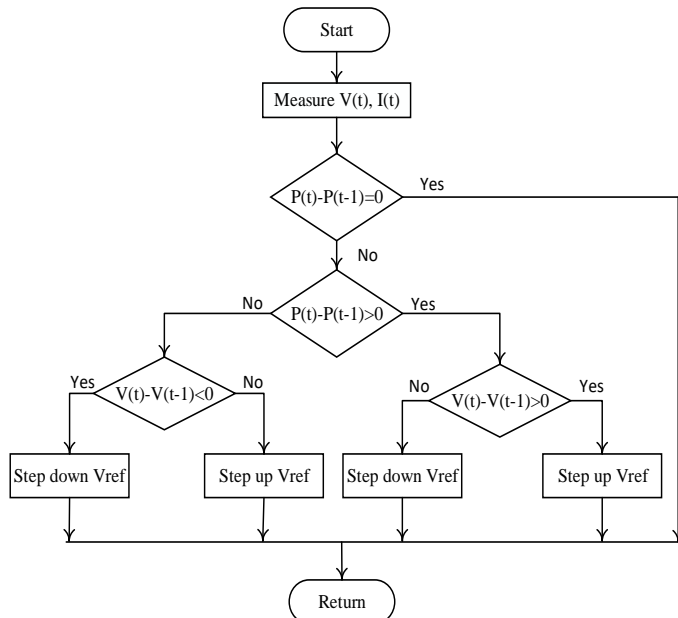


Fig. 7. MPPT flow chart.

### D. Voltage source converter (VSC)

A boosted DC voltage is injected into a three-phase inverter via a DC link capacitor. The three-phase inverter converts the

direct voltage to alternating voltage. The inverter, which used in this work, is simulated by VSC, is suitable for the management of the AC system, because it is controlled in both active and reactive powers simultaneously and separately [9]. The equivalent circuit of VSC is given in Fig. 8 where the control block of the inverter has three input signals, which are DC voltage, reference DC voltage, and AC grid voltages and currents.

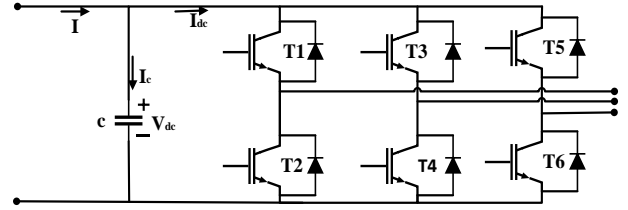


Fig. 8. Equivalent circuit of the VSC [27].

The output of the synchronization control system is firing pulse which controlled in VSC. The frequency and voltage of the AC system are tracked by using a phase-locked loop (PLL) which supplies the inverter with a synchronization signal to get a stable power grid. The measured voltages of the AC system are the inputs of the PLL model, and its output is the phase angle. PLL is designed by using a park transformation to obtain a synchronous  $dq$  reference frame and a PI controller is added to this algorithm as given in (8)-(9). The VSC keeps the DC voltage of the boost converter also it provided with unity power factor [22]. The model is simulated with the DC-voltage controller (the outer controller) which implements by the relation between the obtained value of the reference current and the DC voltage using the PI controller as given in (10). Also, the current regulator (the inner controller) is the difference error among the measured and the referenced value of the current and a PI controller applied for this controller. This controller is used to obtain the  $dq$  reference frame for the voltage of the converter as indicated in (11)-(12) [27].

$$V_d = \frac{2}{3} \left[ V_C * \sin \left( wt + \frac{2\pi i}{3} \right) + V_B * \sin \left( wt - \frac{2\pi i}{3} \right) + V_A * \sin(wt) \right] \quad (8)$$

$$V_q = \frac{2}{3} \left[ V_C * \cos \left( wt + \frac{2\pi i}{3} \right) + V_B * \cos \left( wt - \frac{2\pi i}{3} \right) + V_A * \cos(wt) \right] \quad (9)$$

$$I_{d,ref} = (V_{dc} - V_{dc,ref}) * \left[ K_P + \frac{K_I}{S} \right] \quad (10)$$

$$V_d - V_{d,conv} = \frac{di_d}{dt} + R i_d - \omega L i_q \quad (11)$$

$$V_q - V_{q,conv} = L \frac{di_q}{dt} + R i_q - \omega L i_d \quad (12)$$

where  $V_d$ ,  $V_q$  is the three-phase voltages expressed in two axis  $dq$  reference frame,  $R$ ,  $L$  are the resistance and inductance among the converter and network respectively,  $V_A$ ,  $V_B$ ,  $V_C$  are the measured grid voltages,  $V_{conv}$  is the converter voltages,  $w$  is the angular frequency,  $i_d$ ,  $i_q$  are the three-phase currents

expressed in two axis  $dq$  reference frame,  $I_{d,ref}$  is the reference value of current which is the output of the dc voltage controller,  $V_{dc}$  is the DC voltage,  $K_I$  is the integral regulator gain,  $K_P$  is the proportional regulator gain, and  $V_{dc,ref}$  is the reference DC voltage.

**E. Battery model**

There are many methods to model lead-acid batteries, where depend on the accuracy of the simulation and which parameters are taken into consideration. Some methods need to perform experiments and measure voltage and current during the discharging and charging process to verify the characteristics of the battery [6]. As shown in Fig. 9, an alternative method to the battery model is used as an equivalent circuit.

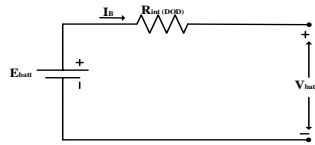


Fig. 9. Equivalent circuit of battery [24].

There is a block in the library of MATLAB/Simulink® which represents the battery [19]. The battery is connected in parallel with the PV system via a bidirectional converter at the same DC bus to keep the DC bus voltage. The process of charging/discharging the battery depends on the value of the DC bus voltage. During high solar power, PV system has the ability to supply the DC bus voltage and charge the connected storage system. But during low solar power, the battery will discharge the required power and provide the DC bus with power to keep the rated voltage. The lead-acid battery is simulated by using the following equations according to the equivalent circuit [24]:

$$V_{batt} = E_{batt} + I_B * R_{int} \tag{13}$$

During discharging mode ( $i^* > 0$ ):

$$f(c, i^*, I_B, Exp) = V_0 - Q \frac{c_{max}}{c_{max} - c} i^* - Q \frac{c_{max}}{c_{max} - c} c + Laplace^{-1} \left( \frac{Exp(s)}{x(s)} * 0 \right) \tag{14}$$

During charging mode ( $i^* < 0$ ):

$$f(c, i^*, I_B, Exp) = V_0 - Q \frac{c_{max}}{0.1c_{max} + c} i^* - Q \frac{c_{max}}{c_{max} - c} c + Laplace^{-1} \left( \frac{Exp(s)}{x(s)} * \frac{1}{S} \right) \tag{15}$$

where,  $V_0$  is the constant voltage(V),  $i^*$  is the output current of low pass filter (A),  $Q$  is the constant polarized resistance ( $\Omega$ ),  $c_{max}$  is the maximum capacity of the battery (Ah),  $c$  is the obtained capacity (Ah).  $I_B$  is the current of battery (A),  $R_{int}$  is the internal resistance of the battery ( $\Omega$ ),  $V_{batt}$  is the output voltage of the battery (V).  $E_{batt}$  is the controlled voltage source (V),  $Exp(s)$  is the exponential zone of voltage (V) . $x(s)$  is the mode of the battery where  $x(s) = 1$  during charging the battery and  $x(s) = 0$  during discharging the battery.

The charging and discharging characteristics of the designed lead-acid battery which uses in this paper are given in Fig. 10 which consists of three parts. The first part describes the voltage dropped exponentially after charging the battery, where the width of this drop is related to the type of battery. The second part describes the steady-state operation of the battery before the voltage drops below the rated voltage of the battery. The third part describes the discharge curve of the battery after the dropping in voltage.

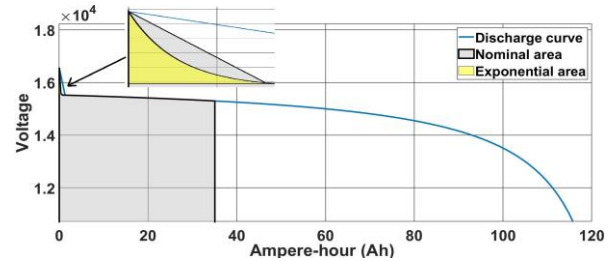


Fig. 10. The characteristics of the lead-acid battery [24].

The charge of the battery is measured by the state of charge (SOC) which is a percentage of the total charge, and the depth of discharge (DOD) which is expressed as a function of (SOC) as shown in the following equations [24]:

$$SOC = \frac{c_{max} - c}{c_{max}} = 1 - \frac{c}{c_{max}} \tag{16}$$

$$DOD + SOC = 100\% \tag{17}$$

The lead-acid battery is simulated in MATLAB/Simulink® according to the equivalent circuit and mathematical equations with the following specifications:

- Nominal voltage :15.3 KV
- Rated capacity :113Ah
- Maximum capacity:117 Ah
- Initial charge :50%
- Internal resistance:0.48673  $\Omega$

**F. SMES model**

Modeling and simulation of SMES can be presented by using different types of power conditioning systems (PCS). There are three main types of PCS can be used with SMES such as current source converter (CSC), voltage source converter (VSC) and thyristors based SMES. In this paper, VSC is used to handle the process of transferring power between the ac system and SMES. Fig. 11 indicates that SMES with VSC contains a superconducting coil and a bidirectional converter which is linked by a DC capacitor with a voltage source converter.

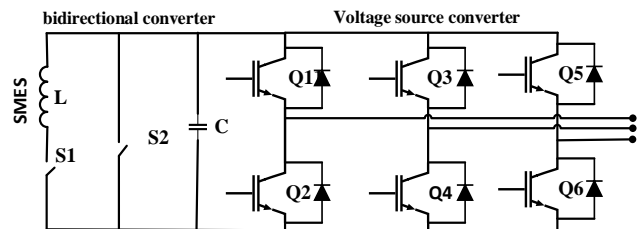


Fig. 11. Schematic diagram of Basic SMES with VSC system [28].

Where the specifications of SMES are defined from both the energy which is stored in the coil and the produced power.

They can be calculated as shown in the following equations [28]:

$$E = \frac{LI^2}{2} \quad (18)$$

$$P = VI = \frac{dE}{dt} = LI \frac{dI}{dt} \quad (19)$$

where I is the current which passes across the coil (A), E is the energy which is stored in the coil (J), P is the nominal power (w). L is the inductance of the coil (H), V is the applied voltage through the coil (V). Where, SMES is used in this paper with the following specifications: inductance of superconducting coil: 8H, the resistance of superconducting coil: 1nΩ, and power rating: 1.35MW

### G. Power system stability indicators

The stability of the power system is defined as the ability of the connected generators to keep in synchronization with the grid. An abnormal state such as switching the loads and faults may cause instability status for the power system. The transient stability can be measured by many factors as follows [13]:

- 1) *The maximum deviation in the rotor speed:* is the highest value of variance in the rotor speed of the synchronous generator when a fault is occurred.
- 2) *Drop in the grid voltage:* there is a fall in the voltage of the grid with applying different types of faults in the power system. The network stability is analyzed according to the amount of the drop in this voltage and taking in consideration the required time for the terminal voltage to back to the nominal value after cleaning the fault.
- 3) *The duration of the oscillation:* is the required time for the system to be in equilibrium state after cleaning the fault.

All these factors are used in this paper to indicate the effect of DG and storage on system stability.

### III. ANALYSIS PROCEDURE

The transient stability of the tested distribution system is analyzed according to these steps, and as shown in Fig.12.

1. Model the tested distribution system without DGs under steady-state operating conditions.
2. At a selected time, a fault is occurred at a selected bus and is removed at a defined time [13].
3. The stability of the system is analyzed during the fault according to the maximum deviation in rotor speed and the drop in voltages.
4. The previous procedures are repeated after injecting PV at the selected bus without any storage devices.
5. Conventional batteries are connected with the same DC bus of PV and repeats that test.
6. SMES is connected with PV at the DC bus and the performance of the system is studied.
7. All the previous steps are repeated with the different types of faults.

### IV. CASE STUDIES AND RESULTS

Transient disturbances like switching operations and faults are very important to study. These disturbances influence the rotor speed deviation, frequency, grid voltage, and rotor angle stability. Rotor speed deviation and the drop in the grid voltages are used in this paper to indicate the effect of the PV system and ESS on the stability of the radial distributed 8-bus system as indicated in Fig. 13, Fig. 14 and Table I. Many scenarios are listed to analyze the impact of solar cells and ESS on the stability of the system with the three types of faults. The total load is 45MW and 21MAVR. The PV system is integrated into the system with a fixed generation capacity with specifications shown in Table II. It provides with penetration level 30% at bus-4 according to the previous research [13]. where the penetration level of DG is defined from the following equation [16]:

$$\%DG = \frac{\sum P_{DG}}{\sum P_{load}} \quad (20)$$

where  $P_{DG}$  is the overall power produced from DGs and  $P_{load}$  is the whole connected load.

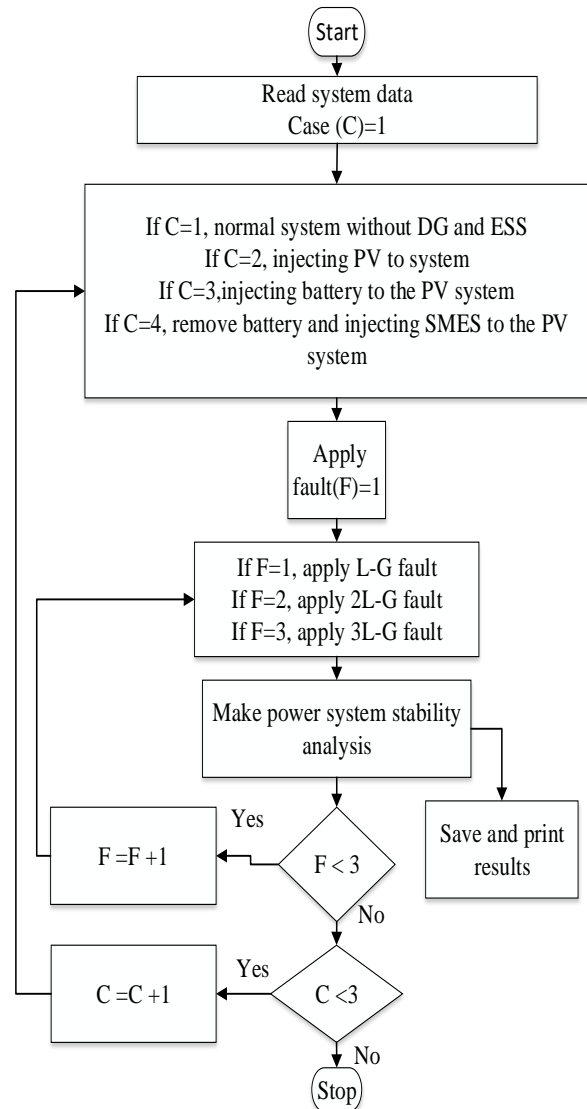


Fig. 12. Transient stability Analysis of Distribution System with DG and storage system

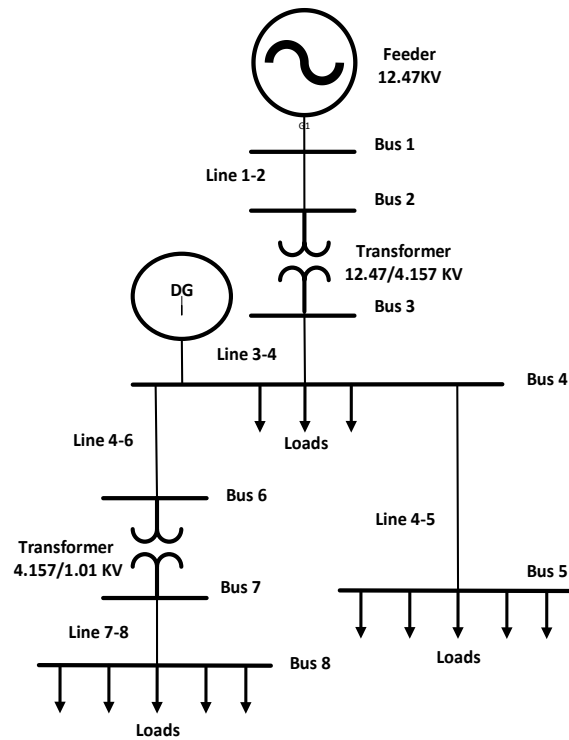


Fig. 13. Radial distributed 8-bus system.

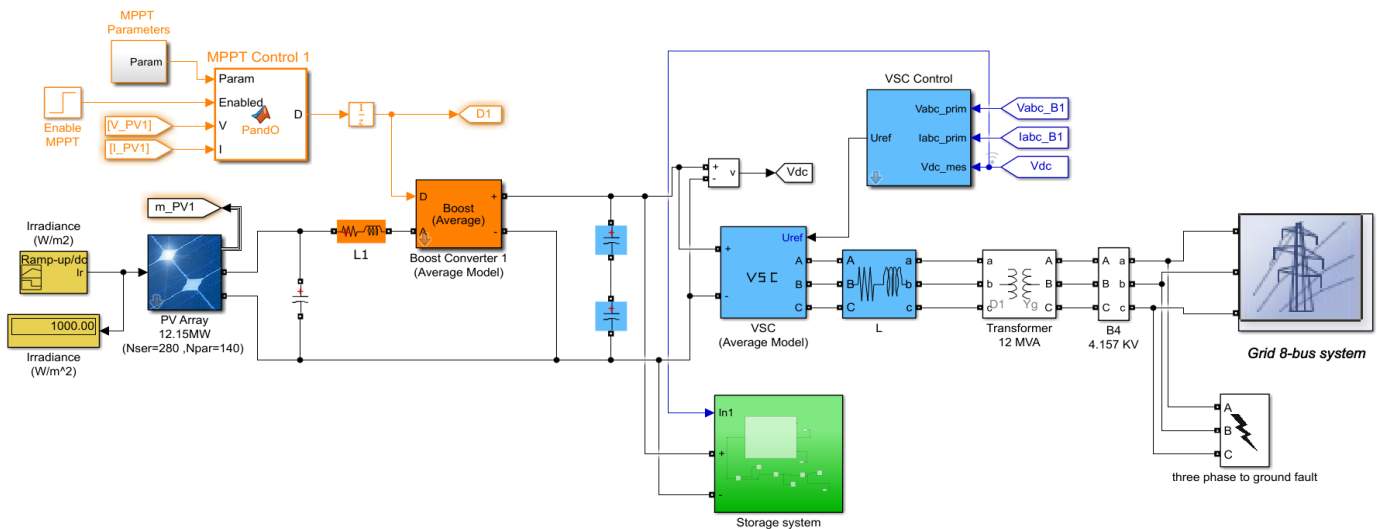


Fig. 14. PV system and storage system connected with grid.

TABLE I  
DETAILED DATA OF THE IEEE 8-BUS SYSTEM

Line Data				Bus	Load Data		Generation Data
From	To	R (Ω)	L (H)		(MW)	(MVAR)	
1	2	2.23081	1.5047	1	-	-	Feeder:12.47KV
3	4	1.68671	1.1377	4	15	7	penetration level of PV is 20% &penetration level of storage system is 10% at bus-4.
4	5	1.9702	0.8074	5	15	7	
4	6	1.0882	0.734	8	15	7	
7	8	1.25143	0.8441	Total	45	21	

TABLE II  
THE PARAMETERS OF THE SOLAR MODEL

Symbol	Parameter	Value
$N_p$	number of parallel solar modules	140
$I_{SC}$	short circuit current (A)	5.96
$V_{OC}$	Open circuit voltage (V)	64.2
$N_s$	number of series cells	280
$M_p$	Maximum power(MW)	12.15

The stability of the system is analyzed with different types of faults according to three indicators :the value of maximum deviation in rotor speed of the synchronous generator, the drop in boosted DC voltage, and the drop in terminal grid voltage.

### 1) The impact of different types of faults:

Three different faults (single line to ground fault, two-line to ground fault, and three-line to a ground fault) are applied at bus 4 at time 4 sec and are cleared at time 5sec. where the effect of each type of faults on the stability of the system either with or without any storage devices is indicated in Fig.15. This figure shows that the maximum deviation in the rotor speed is higher with the three lines to ground fault than the other faults, so the three lines to a ground fault has an enormous effect on the power system stability. Fig. 15 indicates that the maximum rotor speed deviation with the three types of faults is decreased with the addition of battery storage systems and is decreased more when SMES is added to the system, so the obtained results show that energy storage systems are improved the stability of the system.

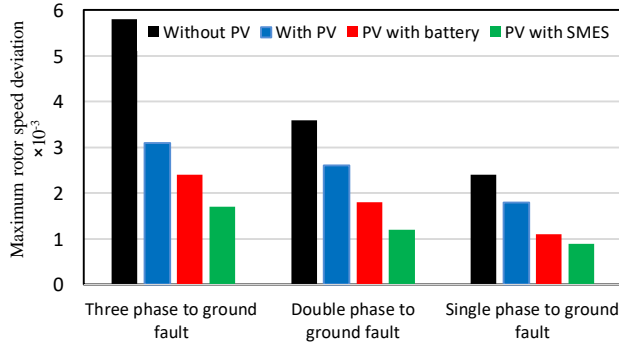


Fig. 15. The maximum rotor speed deviation with different types of faults are applied at bus-4.

### 2) The maximum deviation in the rotor speed:

The rotor speed deviation is analyzed with three types of faults (three-phase to a neutral fault, two phases to a neutral fault, single phase to a neutral fault) are applied at time 4 Sec at bus-4 and cleared after 100ms. As shown in Fig. 16(A), the obtained results with a three-phase to ground fault show that the maximum deviation in the rotor speed increased and reached about 0.0058 when the distribution system without PVs. When the PV system is added to the system, the maximum rotor speed deviation is decreased to 0.0031, and is decreased to 0.0024 with the addition of a battery storage system.

When the battery is replaced with SMES, the maximum rotor speed deviation is decreased more and reached about 0.0017 because SMES has a rapid response and high energy density [9]. The oscillation period of the system is decreased

with the addition of ESS as shown in table III. So the distribution system stability is enhanced during the addition of a photovoltaic system with energy storage devices as shown in Fig. 16.

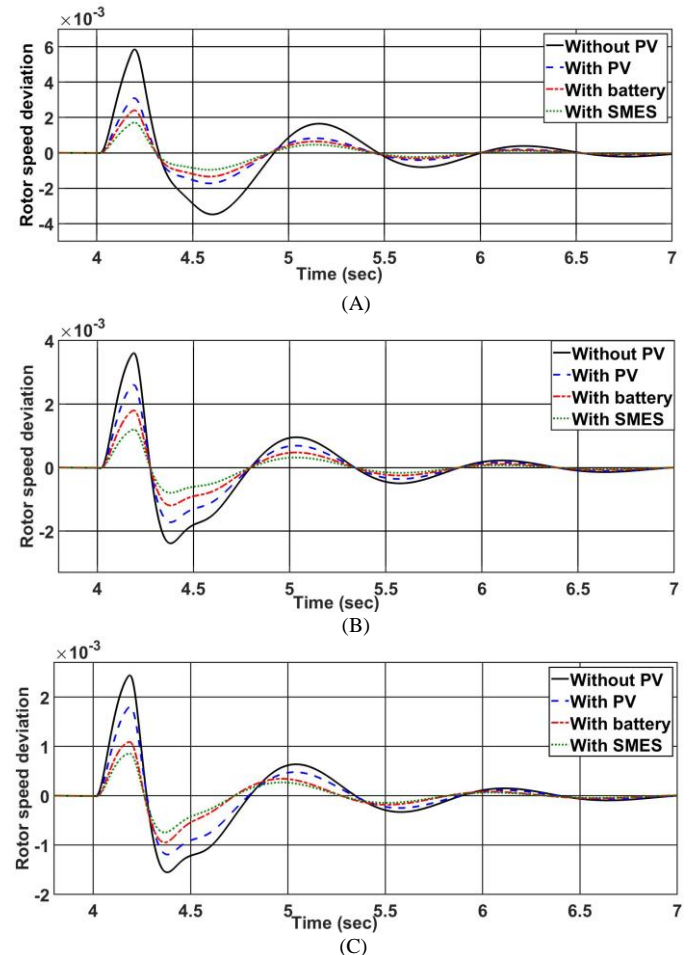


Fig. 16. rotor speed deviation in (PU) (3L-G fault(A), 2L-G fault(B), L-G-fault(C)).

### 3) Drop in DC voltage:

There's a drop in the DC voltage when a fault is applied at time 4 sec and cleared at time 5 sec. where the amount of the drop in the DC voltage is reached about 64 % from the rated voltage with a three-phase to ground fault when the PV system is connected to the distribution system without ESS. This drop is decreased more by adding energy storage systems such as batteries or SMES, as shown in Fig. 17. The performance of the DC voltage is more stable with SMES than battery. As shown in Fig. 17 (A) the amount of drop in the DC voltage is around 22% in case of SMES, and the required time for the DC voltage to be steady-state is less than it when the battery is used. SMES can increase the return efficiency of the system to a steady-state after abnormal changes of energy flow because it has a rapid response (milliseconds) [7].



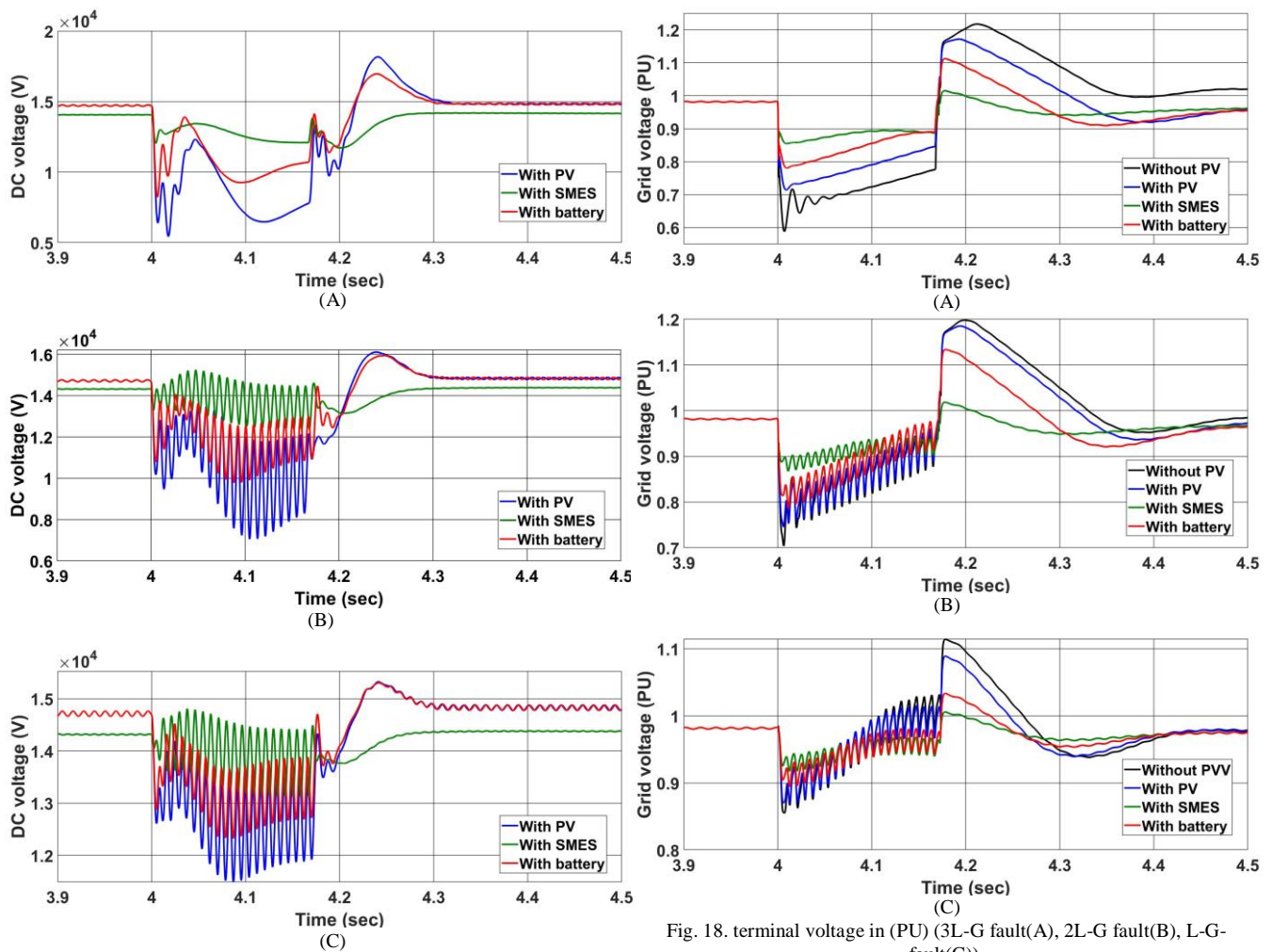


Fig. 17. DC voltage (V) (3L-G fault(A), 2L-G fault(B), L-G-fault(C)).

Fig. 18. terminal voltage in (PU) (3L-G fault(A), 2L-G fault(B), L-G-fault(C)).

4) Terminal voltage:

The drop in the voltage of the grid during fault and the required time for this voltage to return to the nominal voltage after clearing the fault is used to indicate the stability of the system. As shown in Fig.18(A) with a three-line to ground fault, the amount of the drop in the grid voltage is increased and is reached about 42% from the rated voltage during the fault when the system operates without PV. With the addition of the PV system, the amount of the drop in the grid voltage is decreased to 27%. And this drop is decreased more by adding ESS to the system. While the required time for this voltage to return to the rated voltage is decreased more when storage devices such as the SMES are connected at DC bus, but this time is increased when the battery is used. So, the stability of the system is increased when storage devices are added to the PV system.

5) Comparing results:

The results obtained from this paper are compared with the results reported in [13], where the types of energy storage systems which is used in [13] are battery and ultra-capacitor. However, battery and SMES are used in this paper. As shown in Table III, it is observed that the results of the effect a battery on the maximum rotor speed deviation in [13] are compatible with the results obtained in this paper. The results obtained from Fig.15 and table III show that the SMES has a great impact on the maximum deviation in rotor speed and improved the stability of the system during faults.

TABLE III

THE MAXIMUM ROTOR SPEED DEVIATION WITH DIFFERENT TYPES OF FAULTS.

Case Fault Type	The obtained results in this paper						The reported results in [13]	
	With PV		With battery		With SMES		With PV	With battery
	$\Delta N_{max}$	$T_S$	$\Delta N_{max}$	$T_S$	$\Delta N_{max}$	$T_S$		
3L-G fault	0.0031	3.2	0.0024	2.5	0.0017	2.3	0.003	0.0025
2L-G fault	0.0026	3	0.0018	2.3	0.0012	2	0.0027	0.0021
L-G fault	0.0018	2.5	0.0011	2	0.0009	1.8	0.0019	0.0013

## V. CONCLUSION

Adding the DGs to the distribution system reduced many problems caused by renewable sources, but the fluctuating effect of the DG sources still exists but not concentrated in one place. One solution to improve the impact of DGs on the stability of the distribution system is the addition of energy storage systems (ESS). This paper analyzed the effect of adding a PV system with different energy storage devices (battery/SMES) to the radial distributed 8-bus system by using the software program “MATLAB/Simulink®”. The transient stability has been analyzed according to three indicators namely: maximum deviation in the rotor speed and drop in grid voltage during the fault. Different types of the fault have been tested and results showed that 3-phase fault is the most dangerous on system stability. The results have been compared with existing literature under the same conditions and proved the validity of the procedure. The simulation results showed that the energy storage systems have been increased the transient stability of the system. Adding the battery storage system to the distribution system has been decreased the maximum deviation in the rotor speed to 0.0024 and has been reduced the amount of the drop in the grid voltage to 22%. While the maximum deviation in the rotor speed during a fault reached about 0.0017 and the amount of the drop in the grid voltage has been decreased to 14% with the addition of SMES to the photovoltaic system. The comparison between the results obtained using SMES and battery storage show that the SMES has improved the stability of the system in case of abnormal conditions more than the battery, and both increased the stability of the power system.

## References

- [1] M. Ebad, W. Grady, “An approach for assessing high-penetration PV impact on distribution feeders”, *Elec. Power Syst. Res.*, 133, pp. 347-354, 2016.
- [2] k. Honghai, L. Shengqing, W. Zhengqiu, “Discussion on advantages and disadvantages of distributed generation connected to the grid”, *International Conference on Electrical and Control Engineering, China*, 2011, pp.170-173.
- [3] D. Olivares *et al.*, “Trends in microgrid control”, *IEEE Trans. Smart Grid*, vol. 5, no. 4, pp. 1905-1919, Jul. 2014.
- [4] M. Argyrou, P. Christodoulides, S. Kalogirou, “Energy storage for electricity generation and related processes: Technologies appraisal and grid scale applications”, *Renew. Sustain. Energy Rev.*, vol. 94, PP. 804–821, 2018.
- [5] B. Zakeri, S. Syri, “Electrical energy storage systems: a comparative life cycle cost analysis”, *Renew. Sustain. Energy Rev.*, PP. 569-596,2015.
- [6] L. H. Macedo, J. F. Franco, “Optimal Operation of Distribution Networks Considering Energy Storage Devices,” *IEEE Transactions on smart grid* Vol. 6, pp: 2825-2836, 2015.
- [7] A.A.Khodadoost , G.B. Gharehpetian, M.Abedi, “Review on Energy Storage Systems Control Methods in Microgrids”, *International Journal of Electrical Power & Energy Systems*, Vol. 107, May 2019, pp.745-757
- [8] S. Hoshiyar, V. Shelly, “Comparative Analysis Between SMES and BESS in Application of VSC-HVDC System”, *IEEE INDICON* 2015.
- [9] G. Vulusala, V. Suresh, S. Madichetty , “Application of superconducting magnetic energy storage in electrical power and energy systems: a review”, *Int. J. Energy Res.*,42( 2),PP. 358-368, 2018.
- [10] R. Shah, N. Mithulananthan, A. Yome, K. Y. Lee “Impact of Large-Scale PV Penetration on Power System Oscillatory Stability”, *IEEE Energy Society General Meeting - Minneapolis*, pp. 1-7,2010.
- [11] A. Agarwal, “Impact of Increased Penetration of Solar PV on Small Signal Stability of Power System”, *International Journal of Engineering Technology Science and Research IJETS*, vol.2, no.7, pp. 41-50, July 2015.
- [12] S.S. Refaat, H. Abu-Rub; A. P. Sanfilippo, A. Mohamed, “Impact of grid-tied large-scale photovoltaic system on dynamic voltage stability of electric power grids”, *IET Renewable Power Generation*,12, no.2, PP.157-164, Qatar,2017.
- [13] A.K. Srivastava, A.A. Kumar, N.N. Schulz, “Impact of Distributed Generations with Energy Storage Devices on the Electric Grid”, *IEEE Systems Journal*,6, no. 1, pp.110-117, March 2012.
- [14] A. Zahedi, “Maximizing solar PV energy penetration using energy storage technology”, *Renewable and Sustainable Energy Reviews*, Australia,15, no.1, pp.866-870,2011.
- [15] R. Shah; N. Mithulananthan; R.C. Bansal, “Damping performance analysis of battery energy storage system, ultracapacitor and shunt capacitor with large-scale photovoltaic plants”, *Applied Energy*, Australia, vol.96, pp.235-244,2012.
- [16] R. Sharma, M. Singh, D. K. Jain, “Power system stability analysis with large penetration of distributed generation”, *6th IEEE Power India International Conference (PIICON)*, Delhi, India,5-7 December 2014, pp.1-6.
- [17] E. Munkhchuluun, L. Meegahapola, A. Vahidnia, “Impact on Rotor Angle Stability with High Solar-PV Generation in Power Networks”, *IEEE 2017 IEEE PES Innovative Smart Grid Technologies Conference Europe (ISGT-Europe) - Torino, Italy*, 2017, PP.1-6.
- [18] S. Eftekharnajad, V. Vittal, G. T. Heydt, “Impact of Increased Penetration of Photovoltaic Generation on Power Systems”, *IEEE Transaction on power systems*,28, no.2, pp.893-901, May 2013.
- [19] D. Singh, R. Yadav, J. yotsana “Perturb and Observe Method MATLAB Simulink and Design of PV System Using Buck Boost Converter”, *International Journal of Science, Engineering and Technology Research (IJSETR)*, 3, no.6, PP.1692-1696, June 2014.
- [20] B. Mishra, B. PrasannaKar, “Matlab based modeling of photovoltaic array characteristics”, *Department of Electrical Engineering National Institute of Technology, Rourkela, MAY 2012*.
- [21] P. Zarina, M. Sukumar, p. Sekhar, “Photovoltaic system based transient mitigation and frequency regulation”, *Ann. IEEE India Conf. (INDICON)*, 2012, pp.1245-1249.
- [22] R. Song *et al.*, “VSC based HVDC and its Control Strategy”, *IEEE/PES Trans. and Distrb. Conference and Exhibition, Dalian 2005*, pp. 1-6.
- [23] S. S. Mohammed and D. Devaraj, “Simulation and analysis of stand-alone photovoltaic system with boost converter using MATLAB/Simulink,” in *Proceedings of the International Conference on Circuits, Power and Computing Technologies (ICCPCT’14)*, Nagercoil, India, March 2014, pp. 814–821.
- [24] S. Sumathi *et al.*, “Solar PV and Wind Energy Conversion Systems”, *Springer International Publishing Switzerland* 2015.
- [25] S. Sheik, D. Devaraj, T. Imthias, “A novel hybrid Maximum Power Point Tracking Technique using Perturb& Observe algorithm and Learning Automata for solar PV system”, *Energy* 2016, 112, PP.1096–1106.
- [26] R. Moradpur, H. Ardi, A. Tavakoli, “Design and implementation of a new SEPIC-based high step-up DC/DC converter for renewable energy applications”, *IEEE Trans. Ind. Electron.*, 2017, 65, (2), pp. 1290–1297.
- [27] W.Wang, A. Beddard, M. Barnes, “Analysis of active power control for VSC-HVDC”, *IEEE Trans. Power Deliv.*, 2014, 29, (4), pp. 1978–1988.
- [28] K. Saravanan, R. Anita, “Dynamic control modeling and simulation of aUPFC–SMES compensator in power systems”, *Ain Shams Engineering Journal* ,6, PP. 1179–1186, 2015.